PHYSICAL REVIEW B **91**, 121107(R) (2015)

Separability of dynamical and nonlocal correlations in three dimensions

T. Schäfer, A. Toschi, and Jan M. Tomczak*
Institute of Solid State Physics, Vienna University of Technology, A-1040 Vienna, Austria
(Received 23 October 2014; revised manuscript received 11 November 2014; published 16 March 2015)

While second-order phase transitions always cause strong nonlocal fluctuations, their effect on spectral properties crucially depends on the dimensionality. For the important case of three dimensions, we show that the electron self-energy is well *separable* into a local dynamical part and static nonlocal contributions. In particular, our nonperturbative many-body calculations for the three-dimensional Hubbard model at different fillings demonstrate that the quasiparticle weight remains essentially momentum independent, including in the presence of overall large nonlocal corrections to the self-energy. Relying on this insight, we propose a "space-time-separated" scheme for many-body perturbation theory that is up to ten times more efficient than current implementations. Besides these far-reaching implications for state-of-the-art electronic structure schemes, our analysis will also provide guidance to the quest of going beyond them.

DOI: 10.1103/PhysRevB.91.121107 PACS number(s): 71.15.−m, 71.27.+a, 71.30.+h, 74.20.Mn

Introduction. Several iconic phenomena of the many-body problem, such as the Kondo effect or the Mott metal-insulator transition, can be described by *local* correlation effects. This explains the great success of dynamical mean-field theory [1] (DMFT) for our understanding of numerous correlated materials. However, DMFT *ad hoc* assumes the electron self-energy to be independent of momentum. This is known to fail in low dimensions, e.g., for the Luttinger liquid in one dimension (1D) or the strong momentum-space differentiation in (quasi)-2D systems. However, even in three dimensions—the major realm of practical DMFT applications—signatures of nonlocal spatial correlations are apparent, e.g., in the presence of second-order phase transitions. In the 3D Hubbard model, nearest-neighbor spin-spin-correlation functions [2,3], non-mean-field critical exponents [4], and deviations from a local correlations' picture of the entropy [2,3] indicate a paramount effect of nonlocal antiferromagnetic fluctuations in a large region of the phase diagram.

Similarly, for realistic correlated materials, thought to be well described by the combination of density functional theory with DMFT, i.e., DFT + DMFT [5], important nonlocal exchange and correlation effects have recently been established [6–10] within the so-called *GW* approximation [11]—a many-body perturbation theory [12]. Nonlocal effects have, for example, been held accountable for a proper description of the Fermi surfaces in the iron pnictides $BaFe_2As_2$ [6,13] and LiFeAs [6,14], and for the nonmagnetic nature of $BaCo_2As_2$ [15].

Complementary to these manifestations of self-energy effects that are nonlocal in *space*, one might also investigate their structure in the *time* domain. While exchange contributions to the electron self-energy are static by construction, correlation effects are *a priori* both momentum and energy dependent. Recently, it has been proposed that the quasiparticle weight $Z_{\mathbf{k}} = [1 - \partial_\omega \mathrm{Re}\Sigma(\mathbf{k},\omega)]^{-1}_{\omega=0}$, accounting for the low-energy dynamics in the (retarded) self-energy Σ of metals, is essentially momentum independent in the iron pnictides [6], as well as metallic transition-metal oxides [10].

Yet, the basis for the mentioned empirical finding of the locality of $Z_{\mathbf{k}}$ was the weak-coupling *GW* approach, where spin fluctuations are completely neglected. However, large dynamical spin fluctuations have been found in the iron pnictides, both theoretically [16,17] and experimentally [17]. Moreover, these fluctuations were shown to constitute the leading contribution to nonlocal self-energies in the (extended) Hubbard model [4,18,19].

Here, we put the analysis of *nonlocal correlations* in spectral properties of metals on solid grounds. To this aim, we apply a diagrammatic extension of DMFT, the dynamical vertex approximation [20] (DΓA), to the 3D Hubbard model away from half filling. This allows for a precise study of the electron self-energy *beyond* the weak-coupling regime. We find that while nonlocal correlation effects increase substantially when approaching the Mott insulating or the magnetically ordered state, the associated fluctuations do not manifest themselves as a sizable momentum differentiation in the low-energy dynamics of the self-energy. In particular, the quasiparticle weight is indeed found to be essentially local. On the other hand, the momentum variation of the *static* part of the nonlocal self-energy reaches a magnitude of 20% of the half bandwidth, or more. Dynamical renormalizations acquire an appreciable momentum dependence only at energies in the outer half of the quasiparticle bandwidth or higher. We will discuss the implications of our findings for electronic structure schemes and make an explicit suggestion that speeds up self-energy calculations for metals within *GW* by a factor of 10.

Model and method. Our starting point is the 3D Hubbard model on the cubic lattice, $H = -t\sum_{\langle i,j\rangle\sigma} c^\dagger_{i\sigma}c_{j\sigma} + U\sum_i n_{i\uparrow}n_{i\downarrow}$, where $c^\dagger_{i\sigma}$ ($c_{i\sigma}$) creates (destroys) an electron of spin σ at site i, $n_{i\sigma} = c^\dagger_{i\sigma}c_{i\sigma}$, t is the hopping amplitude between nearest neighbor sites $\langle i,j\rangle$, and U is the on-site Hubbard interaction. Our DΓA calculations exploit a DMFT input for the local self-energy and vertex functions [21,22] computed with an exact diagonalization solver and employ the (particle-hole) ladder approximation with Moriya correction in the spin channel [23,25]. Energies will be measured in units of the half bandwidth $W/2 = 6t \equiv 1$. We choose $U = 1.6$, which, at half filling, $n = 1$, yields a Mott insulator with maximal Néel temperature [4]. We thus consider the crossover regime between weak coupling (where the perturbative *GW* approximation is most justified and magnetism is controlled by Fermi-surface instabilities) and the Mott-Heisenberg physics

*Corresponding author: jan.tomczak@tuwien.ac.at

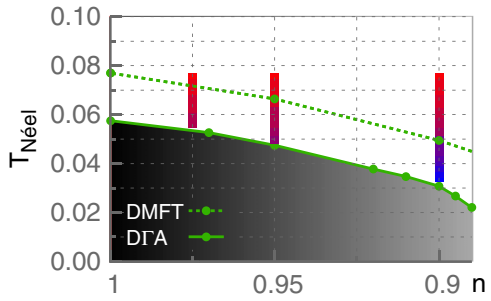

FIG. 1. (Color online) Phase diagram of the 3D Hubbard model within DMFT and DΓA for $U = 1.6$. The solid (dashed) line indicates the DΓA (DMFT) Néel temperature, determined from the divergence of the spin susceptibility. The vertical bars at fixed filling n indicate the temperature paths followed in Fig. 2. The system is Mott insulating at half filling ($n = 1$). All energies measured in units of the half bandwidth.

at large interaction strengths. It was shown (for half filling) that the effect of nonlocal fluctuations is strongest in this intermediate coupling regime [21,23,24].

Results. Figure 1 shows the phase diagram of the 3D Hubbard model as a function of filling n and temperature T. As a clear signature of nonlocal fluctuations, the Néel temperature is reduced by at least 30% in DΓA with respect to the DMFT result. To elucidate the influence of these manifestly nonlocal effects in the *two-particle* antiferromagnetic (AF) susceptibility onto the *one-particle* electronic structure, we analyze the DΓA self-energy when approaching the spin-density wave (SDW) instability at constant filling.

First, we focus on effects near the Fermi level and perform a low-energy expansion of the self-energy: $\Sigma(\mathbf{k},\omega) = \mathrm{Re}\Sigma(\mathbf{k},\omega=0) + [1-1/Z(\mathbf{k})]\omega - \imath\Gamma(\mathbf{k})(\omega^2+\pi^2T^2) + \cdots$, where $\gamma(\mathbf{k}) = -\mathrm{Im}\Sigma(\mathbf{k},\omega=0) = \Gamma(\mathbf{k})\pi^2T^2 + O(T^4)$ is the scattering rate, and $Z(\mathbf{k})$ can be identified as the quasiparticle weight in the Fermi-liquid regime. We recall that in the limit of infinite dimensions, nonlocal self-energy diagrams vanish, and Z and γ are momentum independent [26]. The DMFT self-consistency condition then yields, via Dyson's equation, the exact noninteracting propagator of an effective Anderson impurity problem [1]. In finite dimensions, this is no longer true. Therefore, besides the approximation of assuming the self-energy to be local, this local self-energy does not need to coincide with the local projection of the exact lattice self-energy. In fact, the momentum average $a_{\mathrm{loc}} = 1/N_{\mathbf{k}}\sum_{\mathbf{k}} a(\mathbf{k})$ (with $N_{\mathbf{k}}$ the number of $\mathbf{k}$ points) of the DΓA quasiparticle weight and scattering rate, Z_{loc} and γ_{loc}, deviate notably from the DMFT prediction (Fig. 2, middle and right panels). As expected [20,25], the inclusion of antiferromagnetic fluctuations reduces the quasiparticle weight Z. We note that the temperature evolution of Z_{loc} and its change in hierarchy (for small T, Z is smallest at low doping, $1-n$; while for high T, Z is largest for small doping) follows the same trends as the inverse of the effective mass of the 3D electron gas [27]. For the chosen parameter set, the scattering rate γ in DMFT is large enough to induce a large violation of the pinning condition $\mathrm{Im}G_{\mathrm{loc}}(\omega=0) = \mathrm{Im}G^{U=0}_{\mathrm{loc}}(\omega=0)$, valid for local self-energies with vanishing imaginary part at the Fermi level [28]. Moreover, the temperature dependence of γ evidently involves corrections [30] to the low-energy Fermi-liquid behavior, as neither DMFT nor DΓA yield a T^2 behavior, and therewith the interpretation of the expansion coefficient Z as quasiparticle weight breaks down. Nevertheless, in the following, we will conventionally indicate as "Fermi surface" the solutions $\mathbf{k}_F$ of the quasiparticle equation, $\det[\mu - \epsilon_{\mathbf{k}} - \mathrm{Re}\Sigma(\mathbf{k},0)] = 0$, with the chemical potential μ and the one-particle dispersion $\epsilon_{\mathbf{k}}$ (see Supplemental Material [29]). This can be motivated by the (co)existence of quasiparticlelike excitations, even above the Fermi-liquid coherence scale [30].

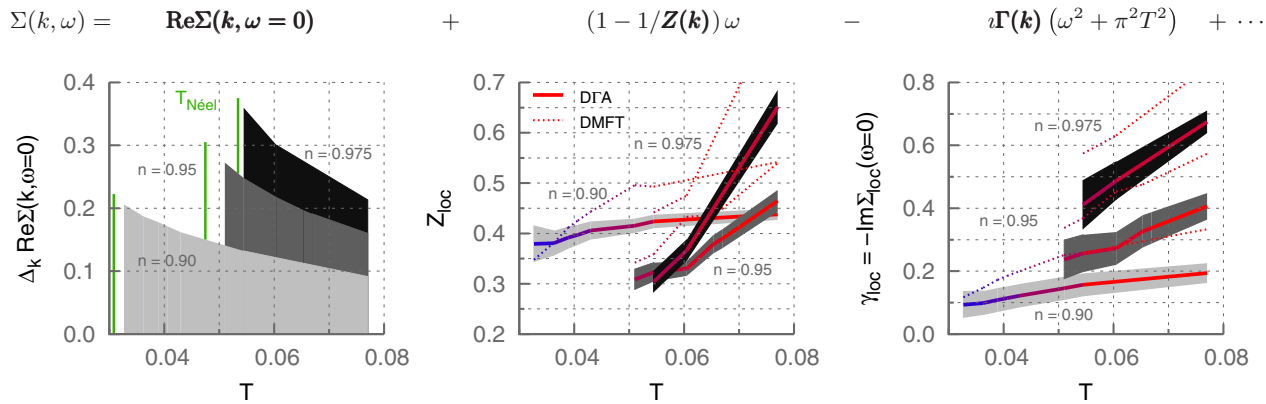

FIG. 2. (Color online) Low-energy expansion of the DΓA self-energy and momentum dependence of the expansion coefficients. The shaded areas (light gray, gray, black) indicate the standard deviation, $\Delta_{\mathbf{k}}a(\mathbf{k}) = \sqrt{1/N_{\mathbf{k}}\sum_{\mathbf{k}}|a(\mathbf{k}) - a_{\mathrm{loc}}|^2}$, of the expansion coefficients $a(\mathbf{k}) = \mathrm{Re}\Sigma(\mathbf{k},\omega=0)$, $Z(\mathbf{k})$, and $\gamma(\mathbf{k}) = -\mathrm{Im}\Sigma(\mathbf{k},\omega=0) = \Gamma(\mathbf{k})\pi^2T^2 + O(T^4)$ in the Brillouin zone with respect to their local values a_{loc}, as a function of temperature for different fillings ($n = 0.9, 0.95, 0.975$). From left to right: (i) The static real part of the self-energy at the Fermi level, $\mathrm{Re}\Sigma(\mathbf{k},\omega=0)$. Its standard deviation increases notably on approaching the Néel transition (marked by green lines). The local value of $\mathrm{Re}\Sigma(\mathbf{k},\omega=0)$, including the Hartree term, was absorbed into the chemical potential. (ii) The quasiparticle weight $Z(\mathbf{k})$. (iii) The scattering rate $\gamma(\mathbf{k})$. For (ii) and (iii), the standard deviation with respect to momentum is shown as stripes (shades of gray) around the respective local value, Z_{loc} and γ_{loc}, within DΓA (solid lines). As a comparison, the (by construction) local values of Z and γ within DMFT are shown (dotted lines). $U = 1.6$ and the temperatures and fillings correspond to the vertical cuts shown in Fig. 1.

In DΓA, the spectral weight at the Fermi level is further depleted compared to DMFT (see Supplemental Material [29] and Refs. [4,20]) and effective masses are reduced (see below). Hence, the *local* electron-electron scattering contributions to quasiparticle lifetimes decrease, explaining why $\gamma^{DMFT} > \gamma_{\rm loc}^{D\Gamma A}$. When approaching the SDW state, however, nonlocal spin fluctuations provide an additional scattering mechanism: While $\gamma \to 0$ for $T \to 0$ in DMFT, the inverse lifetime in DΓA levels off. Concomitantly, and analogous to the incoherence crossover at high T via local electron-electron scattering, the emerging low-T scattering in DΓA causes $Z^{D\Gamma A}$ to saturate towards the SDW state.

We now analyze the momentum dependence of the self-energy by calculating the standard deviation of the expansion coefficients, $a(\mathbf{k}) = \mathrm{Re}\Sigma(\mathbf{k},\omega = 0)$, $Z(\mathbf{k})$, and $\gamma(\mathbf{k})$, with respect to their local values: $\Delta_{\mathbf{k}} a(\mathbf{k}) = \sqrt{1/N_{\mathbf{k}} \sum_{\mathbf{k}} |a(\mathbf{k}) - a_{\rm loc}|^2}$ (see Ref. [6] and Supplemental Material [29]). We find that nonlocal fluctuations manifest themselves very differently in the individual coefficients as follows (from left to right in Fig. 2):

(i) The momentum dependence of the *static* part of the self-energy $\mathrm{Re}\Sigma(\mathbf{k},\omega = 0)$, as measured by the above standard deviation, increases substantially towards the spin-ordered phase, and grows sharply when approaching the Mott insulator at half filling; $\Delta_{\mathbf{k}}\mathrm{Re}\Sigma(\mathbf{k},\omega = 0)$ reaches values as large as 20–40% of the half bandwidth $W/2$—a large effect that is fully neglected in DMFT.

(ii) The standard deviation in momentum space of the quasiparticle weight, $\Delta_{\mathbf{k}} Z(\mathbf{k})$ [depicted as shaded areas around the local values in Fig. 2(b)], is small in all considered cases. Indeed, the largest absolute deviation amounts to only 0.07. In particular, $\Delta_{\mathbf{k}} Z(\mathbf{k})$ does not dramatically increase upon approaching the Néel temperature, in stark contrast to the discussed static part of the self-energy.

(iii) The momentum dependence of the scattering rate γ, shown in Fig. 2(c), remains always moderate. Specifically, the momentum variation increases on absolute values when approaching the Mott insulator at half filling, although the relative importance $\Delta_{\mathbf{k}}\gamma(\mathbf{k})/\gamma$ actually decreases.

In all, we thus find that while spin and charge fluctuations, which develop upon approaching the spin-ordered or Mott-insulating state (see Supplemental Material [29]), can significantly renormalize the value of the quasiparticle weight Z, they do not introduce any sizable momentum differentiation in it. This is in strong opposition to the pronounced nonlocal effects in the static part of the self-energy. The latter will, however, strongly modify the mass m^* of the quasiparticles, as, e.g., extracted from Shubnikov–de Haas or photoemission experiments. Indeed, the effective mass enhancement m^*/m is defined by the ratio of group velocities of the noninteracting and interacting system, respectively,

$$\left(\frac{m^*}{m}\right)^{-1}\Bigg|_{\mathbf{k}_F} = Z(\mathbf{k}_F)\left[1 + \frac{\mathbf{e}_{\mathbf{k}_F}\cdot\nabla_k \mathrm{Re}\Sigma(\mathbf{k},\omega=0)}{\mathbf{e}_{\mathbf{k}_F}\cdot\nabla_k \epsilon_{\mathbf{k}}}\right]_{\mathbf{k}=\mathbf{k}_F}, \tag{1}$$

where $\epsilon_{\mathbf{k}}$ is the noninteracting dispersion and $\mathbf{e}_{\mathbf{k}_F}$ is the unit vector perpendicular to the Fermi surface for a given $\mathbf{k}_F$. Thus, besides the enhancement of m^* via Z (which we showed to be quasilocal; see also Table I), there is a contribution to m^* from the momentum dependence of the static self-energy. The sign of the derivative $\nabla_k \mathrm{Re}\Sigma$ is always positive, thus the effect of nonlocal correlations is to *reduce* the effective mass. In Table I, we give the individual components to m^*/m for three Fermi vectors $\mathbf{k}_F$ [on the Fermi surface, Z and γ are maximal (minimal) for $\mathbf{k}_2$ ($\mathbf{k}_3$)]. We find m^*/m to be notably momentum dependent: $m^*/m = 1.4$ for $\mathbf{k}_1$, while for $\mathbf{k}_3$, $m^*/m = 1.8$—a value larger by 30%. However, it is dominantly the *spatial* variation of the self-energy ($\nabla_k \mathrm{Re}\Sigma$), not a nonlocal dependence in its dynamics (Z), that causes this momentum differentiation. Depending on $\mathbf{k}_F$, nonlocal correlation effects reduce the effective mass down to 55–75% of its dynamical contribution, $1/Z$. In realistic *GW* calculations, even larger reductions were found for iron pnictides [6]. Besides the change in the (local) quasiparticle weight, this is a second, significant effect not accounted for in local approaches, such as DMFT.

TABLE I. Effective masses on the Fermi surface. Contributions to m^*/m from dynamical [Z] and static [$\nabla_k \mathrm{Re}\Sigma(\mathbf{k},0)$] renormalizations for three $\mathbf{k}_F$; see also Fig. 3. In DMFT, $m^*/m = 1/Z = 1/0.44 = 2.26$. $U = 1.6$, $T = 0.043$.

$\mathbf{k} = \mathbf{k}_F$	k_0	$\nabla_k \epsilon_{\mathbf{k}}$	$\nabla_k \mathrm{Re}\Sigma(\mathbf{k},0)$	Z	$1/Z$	m^*/m
$\mathbf{k}_1 = (k_0,k_0,0)$	2.16	0.55	0.30	0.45	2.20	1.42
$\mathbf{k}_2 = (k_0,0,\pi)$	$\pi/2$	0.67	0.20	0.45	2.23	1.72
$\mathbf{k}_3 = (k_0,k_0,k_0)$	$\pi/2$	0.99	0.35	0.41	2.44	1.81

Having so far concentrated on effects at the Fermi level, a natural question arises: Up to which energy scale do dynamical correlations remain essentially local? Figure 3 shows the Fermi surface within DΓA for $n = 0.9$ and the real parts of the self-energies [31] along a path in the Brillouin zone. Congruent with the quasiparticle weight being quasilocal, the slopes of the self-energies at the Fermi level are the same for all momenta and the curves differ by a static shift only. To quantify this observation, we plot in Fig. 3 (right) the standard deviation $\Delta_{\mathbf{k}} Z(\mathbf{k},\omega)$, where we have formally extended the Z factor to finite frequencies: $Z(\mathbf{k},\omega) = 1/[1 - \partial_\omega \mathrm{Re}\Sigma(\mathbf{k},\omega)]$. $\Delta_{\mathbf{k}} Z(\mathbf{k},\omega)$, a measure for the momentum dependence of dynamical correlations, is negligible in the energy window $[-0.25 : 0.6]$. Given the bandwidth renormalization $W \to Wm/m^*$, with the above effective mass ratio, nonlocal correlations are effectively static over most of the *interacting* quasiparticle dispersion.

In Fig. 3, we also show *GW* results: While the slope of the self-energy is constant throughout the Brillouin zone within the linear Fermi-liquid regime (the extension of which *GW* overestimates), the static part shows only a weak momentum dependence also [32]. The comparatively large variations of $\mathrm{Re}\Sigma(\mathbf{k},\omega = 0)$ in DΓA therefore emphasize the pivotal influence of spin fluctuations (neglected by *GW*) onto (static) nonlocal correlations.

Discussion and outlook. The central findings of our analysis for correlated metals in 3D are as follows: (1) Within most of the quasiparticle bandwidth, *nonlocal* correlations are static. Conversely, dynamical correlations are *local*. Hence, the self-energy is *separable* into nonlocal and dynamical contributions,

$$\Sigma(\mathbf{k},\omega) = \Sigma^{\rm nonloc}(\mathbf{k}) + \Sigma^{\rm loc}(\omega), \tag{2}$$

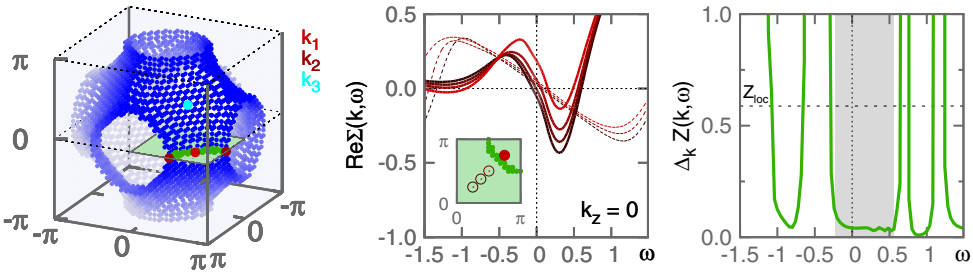

FIG. 3. (Color online) DΓA Fermi surface and momentum dependence of the self-energy. Shown is the Fermi surface computed in DΓA for $n = 0.9$, $U = 1.6$, $T = 0.043$ (left). There, the green square indicates the cut of the Brillouin zone that contains the path $(k,k,0)$ for which the real parts of the DΓA self-energies (middle panel) are shown. Indicated are also the $\mathbf{k}$ points of Table I. The maximal (minimal) Z and γ on the Fermi surface occur at $\mathbf{k}_2$ ($\mathbf{k}_3$). We also show self-energy results from the GW approach (thin dashed lines): GW overestimates Z and the energetic extent of the (linear) Fermi-liquid regime. The right panel shows the standard deviation $\Delta_{\mathbf{k}} Z(\mathbf{k},\omega)$ for the generalized quasiparticle weight $Z(\mathbf{k},\omega) = 1/[1 - \partial_\omega \mathrm{Re}\Sigma(\mathbf{k},\omega)]$: Its momentum variation is negligible with respect to its local value within the gray-shaded energy range that encompasses most of the quasiparticle bandwidth.

providing an *a posteriori* justification for the application of a DMFT-like method to describe $\Sigma^{\mathrm{loc}}(\omega)$ in 3D. We stress, however, that since, e.g., $Z^{DMFT} \neq Z^{D\Gamma A}_{\mathrm{loc}}$, ways to improve the DMFT impurity propagator [e.g., by incorporating $\Sigma^{\mathrm{nonloc}}(\mathbf{k})$ in the DMFT self-consistency] need to be pursued. (2) *Static* correlations have a large momentum dependence, calling for a description of Σ^{nonloc} beyond, say, DFT. This can, e.g., be achieved with the GW+DMFT approach [7,33] or the recently proposed quasiparticle self-consistent (QS)GW+DMFT [6,34]. Exploiting Eq. (2), these can be simplified, as is the strategy in DMFT@(nonlocal GW) [10]. Yet, already the GW can profit: Here we propose to replace Hedin's $\Sigma_{GW}(\mathbf{k},\omega) = 1/N_{\mathbf{q}} \sum_{\mathbf{q},\nu} G(\mathbf{k}+\mathbf{q},\omega+\nu)W(\mathbf{q},\nu)$ with $\widetilde{\Sigma}_{GW}(\mathbf{k},\omega) = \Sigma^{\mathrm{loc}}_{GW}(\omega) + \Sigma^{\mathrm{nonloc}}_{GW}(\mathbf{k})$, where $\Sigma^{\mathrm{loc}}_{GW}(\omega) = \sum_\nu G^{\mathrm{loc}}(\omega+\nu)W^{\mathrm{loc}}(\nu)$, $\Sigma^{\mathrm{nonloc}}_{GW}(\mathbf{k}) = 1/N_{\mathbf{q}} \sum_{\mathbf{q},\nu} G(\mathbf{k}+\mathbf{q},\nu)W(\mathbf{q},\nu) - \Sigma^{\mathrm{loc}}_{GW}(\omega=0)$ for GW calculations of metals. We shall refer to this physically motivated scheme as "space-time-separated GW." Avoiding the $\mathbf{q}$ and ω convolution, respectively, reduces the numerical expenditure from $N_{\mathbf{k}}N_{\mathbf{q}} \times N_\omega N_\nu$ to $N_\omega N_\nu + N_{\mathbf{k}}N_{\mathbf{q}} \times N_\nu$, typically gaining more than an order of magnitude [35]. If the dominant nonlocal self-energy derives from *exchange* effects, Eq. (2) holds and screened exchange (SEx)+DMFT [15] can be employed. In the (one-band) Hubbard model, however, nonlocal self-energies are not exchange driven. Still, as we have shown, Σ^{nonloc} is significant, and in particular beyond a perturbative technique such as GW. Consequently, at least in the vicinity of second-order phase transitions, a methodology beyond (QS)GW+DMFT is required. *Ab initio* DΓA [36] or realistic applications of other diagrammatic extensions [37–41] of DMFT might provide a framework for this. That Eq. (2) holds *beyond* weak coupling, however, nourishes the hope that a much less sophisticated electronic structure methodology can be devised in 3D.

Nonlocal renormalizations that are dynamical occur in lower dimensions, as, e.g., shown theoretically for 2D [41–45]. However, also in 3D, momentum-dependent quasiparticle weights can be generated. In fact, this is the typical situation in heavy fermion systems below their (lattice) Kondo temperature. There, the hybridization amplitude for spin singlets between atomiclike f states and conduction electrons is modulated on the Fermi surface, as it can be rationalized with mean-field techniques [46]. Thus, even a local quasiparticle weight of the f states yields a momentum-space anisotropy of Z via the change in orbital character. This effect has also been held responsible for anisotropies in some Kondo insulators [47]. Beyond this scenario, however, strong intersite fluctuations in the periodic Anderson model [48] suggest actual nonlocal correlation effects to be of crucial relevance to heavy fermion quantum criticality [49,50]. A further source of nontrivial nonlocal correlation effects in 3D are multipolar Kondo liquids [51–53]. To elucidate the latter two phenomena, an application of DΓA to, e.g., the periodic Anderson model is called for.

Acknowledgments. We acknowledge financial support from the Austrian Science Fund (FWF) through Project No. I-597-N16 within the German Research Foundation (DFG) unit FOR 1346. T.S. was supported by the FWF through the Doctoral School Building Solids for Function (Project ID No. W1243). Calculations have been performed on the Vienna Scientific Cluster (VSC).

[1] A. Georges, G. Kotliar, W. Krauth, and M. J. Rozenberg, Rev. Mod. Phys. **68**, 13 (1996).
[2] S. Fuchs, E. Gull, L. Pollet, E. Burovski, E. Kozik, T. Pruschke, and M. Troyer, Phys. Rev. Lett. **106**, 030401 (2011).
[3] E. Kozik, E. Burovski, V. W. Scarola, and M. Troyer, Phys. Rev. B **87**, 205102 (2013).
[4] G. Rohringer, A. Toschi, A. Katanin, and K. Held, Phys. Rev. Lett. **107**, 256402 (2011).
[5] G. Kotliar, S. Y. Savrasov, K. Haule, V. S. Oudovenko, O. Parcollet, and C. A. Marianetti, Rev. Mod. Phys. **78**, 865 (2006).
[6] J. M. Tomczak, M. van Schilfgaarde, and G. Kotliar, Phys. Rev. Lett. **109**, 237010 (2012).
[7] J. M. Tomczak, M. Casula, T. Miyake, F. Aryasetiawan, and S. Biermann, Europhys. Lett. **100**, 67001 (2012).
[8] T. Miyake, C. Martins, R. Sakuma, and F. Aryasetiawan, Phys. Rev. B **87**, 115110 (2013).
[9] R. Sakuma, C. Martins, T. Miyake, and F. Aryasetiawan, Phys. Rev. B **89**, 235119 (2014).
[10] J. M. Tomczak, M. Casula, T. Miyake, and S. Biermann, Phys. Rev. B **90**, 165138 (2014).

[11] L. Hedin, Phys. Rev. **139**, A796 (1965).
[12] G. Onida, L. Reining, and A. Rubio, Rev. Mod. Phys. **74**, 601 (2002).
[13] V. Brouet, P.-H. Lin, Y. Texier, J. Bobroff, A. Taleb-Ibrahimi, P. Le Fèvre, F. Bertran, M. Casula, P. Werner, S. Biermann *et al.*, Phys. Rev. Lett. **110**, 167002 (2013).
[14] S. V. Borisenko, V. B. Zabolotnyy, D. V. Evtushinsky, T. K. Kim, I. V. Morozov, A. N. Yaresko, A. A. Kordyuk, G. Behr, A. Vasiliev, R. Follath *et al.*, Phys. Rev. Lett. **105**, 067002 (2010).
[15] A. van Roekeghem, T. Ayral, J. M. Tomczak, M. Casula, N. Xu, H. Ding, M. Ferrero, O. Parcollet, H. Jiang, and S. Biermann, Phys. Rev. Lett. **113**, 266403 (2014).
[16] A. Toschi, R. Arita, P. Hansmann, G. Sangiovanni, and K. Held, Phys. Rev. B **86**, 064411 (2012).
[17] M. Liu, L. W. Harriger, H. Luo, M. Wang, R. A. Ewings, T. Guidi, H. Park, K. Haule, G. Kotliar, S. M. Hayden, and P. Dai, Nat. Phys. **8**, 376 (2012).
[18] T. Ayral, P. Werner, and S. Biermann, Phys. Rev. Lett. **109**, 226401 (2012).
[19] T. Ayral, S. Biermann, and P. Werner, Phys. Rev. B **87**, 125149 (2013).
[20] A. Toschi, A. A. Katanin, and K. Held, Phys. Rev. B **75**, 045118 (2007).
[21] G. Rohringer, A. Valli, and A. Toschi, Phys. Rev. B **86**, 125114 (2012).
[22] T. Schäfer, G. Rohringer, O. Gunnarsson, S. Ciuchi, G. Sangiovanni, and A. Toschi, Phys. Rev. Lett. **110**, 246405 (2013).
[23] K. Held, A. A. Katanin, and A. Toschi, Prog. Theor. Phys. Supp. **176**, 117 (2008).
[24] E. Gull, P. Staar, S. Fuchs, P. Nukala, M. S. Summers, T. Pruschke, T. Schulthess, and T. Maier, Phys. Rev. B **83**, 075122 (2011).
[25] A. A. Katanin, A. Toschi, and K. Held, Phys. Rev. B **80**, 075104 (2009).
[26] W. Metzner and D. Vollhardt, Phys. Rev. Lett. **62**, 324 (1989).
[27] Y. Zhang and S. Das Sarma, Phys. Rev. B **70**, 035104 (2004).
[28] E. Müller-Hartmann, Z. Phys. B **76**, 211 (1989).
[29] See Supplemental Material at http://link.aps.org/supplemental/10.1103/PhysRevB.91.121107 for details. The Supplemental Material includes Refs. [56–63].
[30] X. Deng, J. Mravlje, R. Zitko, M. Ferrero, G. Kotliar, and A. Georges, Phys. Rev. Lett. **110**, 086401 (2013).
[31] The self-energies are analytically continued to real frequencies by Padé approximants. Owing to a limited precision, kinks [54] and the effective Kondo scale [55] are not discussed.
[32] In *ab initio GW* calculations, the momentum dependence is much larger, owing to long-range (screened) interactions and exchange effects [9].
[33] S. Biermann, F. Aryasetiawan, and A. Georges, Phys. Rev. Lett. **90**, 086402 (2003).
[34] J. M. Tomczak, J. Phys.: Conf. Ser. **592**, 012055 (2015).
[35] Locality (e.g., in G^{loc}) is defined with respect to a local/Wannier basis, $\psi_{L\mathbf{R}}(\mathbf{r})$. This is different from the Coulomb-hole screened exchange (COHSEX) approximation [11] that assumes point locality, $\mathbf{r} = \mathbf{r}'$, for correlations and is, moreover, static for both exchange and correlation contributions to the self-energy.
[36] A. Toschi, G. Rohringer, A. Katanin, and K. Held, Ann. Phys. **523**, 698 (2011).
[37] A. N. Rubtsov, M. I. Katsnelson, and A. I. Lichtenstein, Phys. Rev. B **77**, 033101 (2008).
[38] H. Hafermann, G. Li, A. N. Rubtsov, M. I. Katsnelson, A. I. Lichtenstein, and H. Monien, Phys. Rev. Lett. **102**, 206401 (2009).
[39] C. Slezak, M. Jarrell, Th. Maier, and J. Deisz, J. Phys. Condens. Mat. **21**, 435604 (2009).
[40] G. Rohringer, A. Toschi, H. Hafermann, K. Held, V. I. Anisimov, and A. A. Katanin, Phys. Rev. B **88**, 115112 (2013).
[41] C. Taranto, S. Andergassen, J. Bauer, K. Held, A. Katanin, W. Metzner, G. Rohringer, and A. Toschi, Phys. Rev. Lett. **112**, 196402 (2014).
[42] A. N. Rubtsov, M. I. Katsnelson, A. I. Lichtenstein, and A. Georges, Phys. Rev. B **79**, 045133 (2009).
[43] M. Civelli, M. Capone, S. S. Kancharla, O. Parcollet, and G. Kotliar, Phys. Rev. Lett. **95**, 106402 (2005).
[44] T. Maier, M. Jarrell, T. Pruschke, and M. H. Hettler, Rev. Mod. Phys. **77**, 1027 (2005).
[45] T. Schäfer, F. Geles, D. Rost, G. Rohringer, E. Arrigoni, K. Held, N. Blümer, M. Aichhorn, and A. Toschi, Phys. Rev. B **91**, 125109 (2015).
[46] P. Ghaemi, T. Senthil, and P. Coleman, Phys. Rev. B **77**, 245108 (2008).
[47] H. Ikeda and K. Miyake, J. Phys. Soc. Jpn. **65**, 1769 (1996).
[48] D. Tanasković, K. Haule, G. Kotliar, and V. Dobrosavljević, Phys. Rev. B **84**, 115105 (2011).
[49] Q. Si and F. Steglich, Science **329**, 1161 (2010).
[50] S. Paschen and J. Larrea J., J. Phys. Soc. Jpn. **83**, 061004 (2014).
[51] P. Ghaemi and T. Senthil, Phys. Rev. B **75**, 144412 (2007).
[52] H. Weber and M. Vojta, Phys. Rev. B **77**, 125118 (2008).
[53] J. Won Rhim and J. Hoon Han, J. Phys. Soc. Jpn. **82**, 104704 (2013).
[54] K. Byczuk, M. Kollar, K. Held, Y. F. Yang, I. A. Nekrasov, T. Pruschke, and D. Vollhardt, Nat. Phys. **3**, 168 (2007).
[55] K. Held, R. Peters, and A. Toschi, Phys. Rev. Lett. **110**, 246402 (2013).
[56] K. Held, in *Autumn School on Correlated Electrons. DMFT at 25: Infinite Dimensions*, edited by E. Pavarini, E. Koch, D. Vollhardt, and A. Lichtenstein, Reihe Modeling and Simulation, Lecture Notes Vol. 4 (Forschungszentrum Jülich, Jülich, 2014), available as arXiv:1411.5191.
[57] N. E. Bickers, D. J. Scalapino, and S. R. White, Phys. Rev. Lett. **62**, 961 (1989); V. Janiš, J. Phys.: Condens. Matter **10**, 2915 (1998); Phys. Rev. B **60**, 11345 (1999); D. Senechal *et al.*, *Theoretical Methods for Strongly Correlated Electrons* (Springer, Berlin, 2003), Chap. 6.
[58] K.-M. Tam, H. Fotso, S.-X. Yang, T.-W. Lee, J. Moreno, J. Ramanujam, and M. Jarrell, Phys. Rev. E **87**, 013311 (2013).
[59] S. X. Yang, H. Fotso, J. Liu, T. A. Maier, K. Tomko, E. F. D'Azevedo, R. T. Scalettar, T. Pruschke, and M. Jarrell, Phys. Rev. E **80**, 046706 (2009).
[60] A. Valli, T. Schäfer, P. Thunström, G. Rohringer, S. Andergassen, G. Sangiovanni, K. Held, and A. Toschi, Phys. Rev. B **91**, 115115 (2015).
[61] G. Rohringer, Ph.D. thesis, Vienna University of Technology, 2014.
[62] R. Bulla, T. A. Costi, and D. Vollhardt, Phys. Rev. B **64**, 045103 (2001).
[63] S. Biermann, L. de' Medici, and A. Georges, Phys. Rev. Lett. **95**, 206401 (2005).